THE UNIVERSITY
OF QUEENSLAND
AUSTRALIA

CREATE CHANGE

The University of Queensland Surat Deep Aquifer Appraisal Project (UQ-SDAAP)

Scoping study for material carbon abatement via carbon capture and storage

Supplementary Detailed Report

Multiphase behaviour – relative permeability and capillary pressures

30 April 2019

Authors

Mr Iain Rodger, The University of Queensland
Dr Mohammad Sedaghat, The University of Queensland
Prof Jim Underschultz, The University of Queensland

Citation

Rodger I, Sedaghat M, Underschultz J (2019), Multiphase behaviour – relative permeability and capillary pressures, The University of
Queensland Surat Deep Aquifer Appraisal Project – Supplementary Detailed Report, The University of Queensland.

Referenced throughout the UQ-SDAAP reports as **Rodger et al. 2019b.**

Contents

Tables

Figures

1.   Executive summary

Relative permeability and capillary pressure curves are required for dynamic modelling of carbon dioxide (CO_2) injection. Limited data on relative permeability and capillary pressure is available for the Blocky Sandstone Reservoir, Transition Zone and Ultimate Seal.

Existing relative permeability data suggests that the Blocky Sandstone Reservoir could have low relative permeability to CO_2 (average maximum kr_{CO2} is approximately 0.13) compared to other sandstones, which may limit injectivity.

Capillary pressure data indicates that parts of the Transition Zone will likely act as good membrane seals (intraformational baffles), with Mercury Injection Capillary Pressure (MICP) entry pressures greater than 10,000kPa for some samples. However, significant uncertainty remains around how representative the current relative permeability data is for the deeper areas of the Surat Basin identified as notional injection sector 'sweet-spots'

Reference case relative permeability curves have been defined, and end point scaling used to perform sensitivity analysis.

J functions have been defined in an attempt to represent the variability in the capillary pressure curves anticipated due to geological heterogeneity (particularly in the Transition Zone). Alternate curves will be used for sensitivity analysis

Due to the high uncertainty surrounding these parameters, and their potentially important impacts on any notional CO_2 injection and storage performance, it would be essential to core an appraisal well for special core analysis (SCAL) to be conducted on a range of core samples across the Blocky Sandstone Reservoir, Transition Zone and Ultimate Seal, to better understand (and model) the multiphase behaviour of the CO_2-water system.

2.   Introduction

Supercritical CO_2 behaves quite differently from gaseous CO_2 . This report focusses only on supercritical CO_2 (which is henceforth referred to throughout this report as CO_2). The multiphase behaviour of the CO_2/water system is important for carbon capture and storage (CCS) projects. The shapes and endpoints of relative permeability and capillary pressure curves have important implications for injectivity, plume migration and trapping. These curves (which are required as inputs for numerical flow simulations) are dependent on a number of factors including the shape, size and distribution of the pores and pore throats; the wettability of the system; and the interfacial tension between the two phases. There is an extensive volume of literature on this topic available covering both theory as well as measured data. A small key subset of this literature includes for example Burnside and Naylor 2014, Iglauer et al. 2014 and Krevor et al. 2012. While this background information provides the theoretical context of the key processes and the geological factors that typically impact variations in relative permeability, site specific measurements are required, because the range of possible values based on measured data from analogue sites is extreme.

Given that no well data currently exists in the UQ-SDAAP notional injection sector sweet spots, the project developed an approach to estimate the most likely range of relative permeability values on existing data from the Surat Basin and from the literature. This report describes the approach taken to represent relative permeability and capillary pressures in the UQ-SDAAP dynamic models.

3.   Relative permeability

3.1   Background

Intrinsic (absolute) permeability refers to the ability of a rock to allow fluid to flow through its pore space. The intrinsic permeability is referenced to a fluid type such as air, nitrogen, helium, oil, methane, CO_2 or water assuming that the pore space is 100% saturated with the reference fluid. Effective phase permeability is the permeability *to a specific fluid* taking into account the presence of one or more other immiscible fluid (or fluids) in the pore space. The effective phase permeability of a particular fluid will vary with saturation (i.e. how much of the pore space is occupied by each fluid). The relative permeability for a fluid (k_r) at any specific saturation is the ratio of the effective phase permeability (at that saturation), to the intrinsic permeability of the rock (which is saturation independent).

It is important to note that the relative permeability of a fluid can also vary depending on whether saturation of the non-wetting[1] phase is increasing (drainage) or decreasing (imbibition). Typically, when CO_2 is injected into a water bearing formation with reservoir (rather than seal) characteristics, the CO_2 will act as a non-wetting phase (Burnside and Naylor 2014), and injection will be a drainage process.

For CO_2 injection into an aquifer, the reservoir rock will initially be (very close to) 100% saturated with water (S_w =1). The effective phase permeability to water at this point will be equal to the intrinsic permeability of the rock, so k^d_{rw}[2] would equal to 1. As CO_2 is injected (i.e. drainage), the saturation of water will decrease. The relative permeability to water (k^d_{rw}) will also decrease as an increasing amount of the available pore space becomes occupied by CO_2. This will coincide with an increase in the relative permeability to CO_2 (k^d_{rg}). The relative permeability to water k^d_{rw} decreases towards zero as S_w approaches the irreducible water saturation (S_{wi}) - the saturation at which the remaining water is immobile (Satter et al. 2008). However, S_w may not reach S_{wi} if differential pressures are not sufficiently high, and k^d_{rw} may become effectively zero before S_{wi} is reached. S_w when k^d_{rw} becomes zero is the residual water saturation (S_{wr}) at the specified differential

---

[1] Wettability refers to the tendency of one fluid to remain in contact with a surface in the presence of another (or multiple other) immiscible fluids. The wetting phase is the phase which preferentially remains in contact with the surface, and thus has a contact angle of less than 90°, while the non-wetting phase is the opposite (and will 'bead' on the surface)

[2] The subscript w indicates the water relative permeability, while the superscript d indicates drainage. kr^i_g would refer to the relative permeability to gas (in this case actually supercritical CO_2) during imbibition.

pressure. At this point, S_w cannot be reduced further without increasing the differential pressure, and thus the maximum CO_2 saturation (and maximum k^d_{rg}) is reached.

After injection finishes, fluids will continue to move in the reservoir, particularly if the injection is into an aquifer rather than a structural trap for example. In some places, water will begin to now displace CO_2 within the pore space (imbibition), which will be associated with a reduction in the relative permeability to CO_2 (k^i_{rg}). This will not follow the same relative permeability curve defined for the displacement case because some CO_2 will become trapped within the pore network by snap-off processes leaving a residual saturation of the non-wetting phase that drives relative permeability hysteresis effects. This residually trapped CO_2 occupies a portion of the pore space (i.e. reduces the water saturation) but becomes increasingly immobile and thus reduces k^i_{rg}. Eventually the non-wetting phase residual saturation is reached where k^i_{rg} is equal to zero, and any remaining CO_2 saturation is immobile (it is trapped in the pore space regardless of structural geometry).

The end points of these curves (the residual saturations of water and CO_2, and the relative permeability to the mobile fluid at these saturations), and their shapes (curvature) can be determined through laboratory experiments (Honarpour and Mahmood 1988).

3.2   Relative permeability data from the Blocky Sandstone Reservoir

An extensive vertical profile of both measured and modelled relative permeability data for the CO_2-water system in the Blocky Sandstone Reservoir is available from Lithicon's analysis of core from the West Wandoan 1 well (located in the northern depositional centre on the eastern side of the MAR sector). This analysis is presented in detail in ANLEC 2016 and the modelled relative permeability curves based on unsteady state experiments are shown in Figure 1.

These curves indicate that endpoint CO_2 relative permeabilities are typically in the range of 0.1 to 0.3, with S_{wr} between 0.25 and 0.65. The authors of the original report indicated that the high residual water saturations and low relative permeability endpoint values could be caused by CO_2 bypassing brine during laboratory experiments and by wettability effects, and note that *"measured data do not fully represent the endpoints".*

As well as the uncertainty regarding how well the laboratory data represents the real, in-situ behaviour, there is also some uncertainty around how well the core from West Wandoan 1 represents the Blocky Sandstone Reservoir across the Surat Basin, particularly in the deeper regions considered as notional injection sites (La Croix et al. 2019a, 2019b, 2019c, 2019d; Gonzalez et al. 2019a, 2019b; Harfoush et al. 2019a, 2019b, 2019c, 2019d).

Despite these potential issues, we concluded that the relative permeability curves (and endpoints) used in numerical simulations of CO_2 injection for UQ-SDAAP should be based mainly on the West Wandoan 1 core analysis. This decision was made on the basis that the core analysis represents the only available *real* data for CO_2-water relative permeability in the Blocky Sandstone Reservoir and it falls within the range of values reported in the literature for other analogue sandstones to the Block Sandstone Reservoir.

Figure 1   Drainage relative permeability curves for laboratory measurements on core samples from the Blocky Sandstone Reservoir interval of the West Wandoan 1 well (ANLEC 2016).
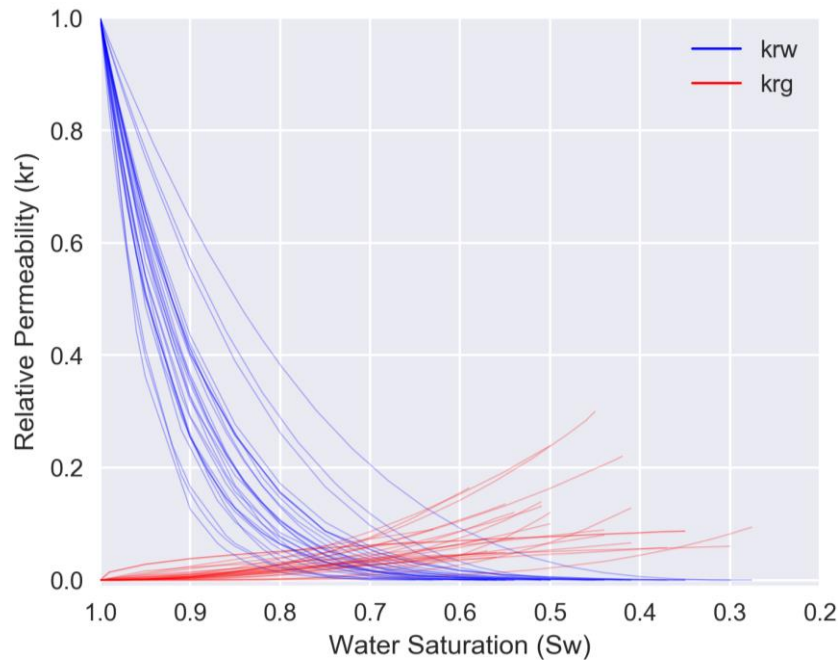
As well as the endpoint at S_{wr} and kr_{gmax}, some plugs were analysed by Lithicon to determine the residual CO_2 saturation (ANLEC 2016). They reported residual CO_2 saturations ranging from 0.15 to 0.76 (*note that this is saturation of CO_2, i.e. S_{CO2} not S_w*) with most plugs giving residual CO_2 saturations between 0.25 and 0.4.

3.3   Relative permeability data from literature

This section presents a brief summary of CO_2-water relative permeability data from literature. We did not directly use the values from literature for CO_2 injection modelling, but include them to allow comparison of the data from the Blocky Sandstone Reservoir with similar data from other analogous sandstone formations. The data presented in this section (as well as data from non-sandstone formations) has been summarised previously, with the implications for CO_2 storage discussed in detail, by Burnside and Naylor 2014. For this reason, we will focus specifically on the comparison of the results from literature with the core data from the West Wandoan 1 well.

Endpoint data (i.e. residual saturations of water and CO_2, and maximum relative permeability to CO_2) from nine studies are shown in Table 1, and S_{wr} and maximum k^d_{rg} values from this table are plotted with the equivalent data from West Wandoan 1 in Figure 2. This suggests that while the maximum relative permeabilities to CO_2 determined in the analysis of the West Wandoan 1 core are relatively low (ranging from 0.04 to 0.30), they are not outside the range of values reported for other formations (ranging from 0.04 to 0.96). Correspondingly, the residual water saturations from West Wandoan 1 are slightly high compared to the literature values but within the range reported.

The residual CO_2 saturations in Table 1 range from 0.10 to 0.51, with most values occurring between 0.2 and 0.38. Again, this appears consistent with the values from the West Wandoan 1 core analysis.

Table 1   *Relative permeability endpoints from nine studies in the literature. Modified from Burnside and Naylor 2014. Note that the project team was unable to find the original references for Mackay et al. 2010 and Shell 2011, and they are reported per Burnside and Naylor 2014.*

Paper	Formation	Maximum Relative Permeability to CO_2 (kr_{gmax})	Residual Saturation of Water (S_{wr})	Residual Saturation of CO_2 (S_{rCO2})
Bennion and Bachu (2008)	Basal Cambrian Fm	0.545	0.294	-
	Ellerslie Fm	0.116	0.659	-
	Viking Fm	0.332	0.558	-
	Viking Fm	0.264	0.423	0.297
	Cardium Fm	0.526	0.200	0.102
	Cardium Fm	0.129	0.420	0.253
Bachu (2013)	Viking Fm	0.097	0.601	0.223
	Clearwater Fm	0.494	0.343	0.145
	Ellerslie Fm	0.574	0.382	0.421
	Rock Creek Fm	0.043	0.479	0.477
	Halfway Fm	0.273	0.466	0.459
	Belloy	0.076	0.653	0.283
	Graminia Fm	0.146	0.442	0.383
	Gilwood Fm	0.545	0.566	0.359
	Basal Cambrian Fm	0.211	0.569	0.234
	Basal Cambrian Fm	0.156	0.490	0.403
	Basal Cambrian Fm	0.210	0.651	0.269
	Basal Cambrian Fm	0.326	0.275	0.519
	Deadwood Fm	0.106	0.490	0.382
	Deadwood Fm	0.094	0.596	0.288
	Deadwood Fm	0.260	0.654	0.238
	Granite Wash	0.405	0.579	0.226
Shi et al. (2011a)	Tako Sandstone	0.135	0.570	0.280
Shi et al. (2011b)	Berea	-	0.687	0.210
Pentland et al. (2011)	Berea	-	0.150	0.350
Perrin and Benson (2010)	Berea	0.063	0.620	-
	Otway Basin	0.608	0.434	-
Krevor et al. (2012)	Berea	0.380	0.450	0.310
	Paaratte	0.300	0.410	0.330
	Mt. Simon	0.460	0.460	0.210
	Tuscaloosa	-	0.540	0.310
Referenced as Mackay et al., (2010) in Burnside and Naylor (2014)	Clashach	0.080	0.380	0.380
	Sherwood	0.061	0.557	0.283
Referenced as Shell (2011) in Burnside and Naylor (2014)	Captain	0.960	0.330	0.380
	Captain	0.920	0.300	0.290

Figure 2   Drainage CO$_2$ relative permeability endpoint data from literature (triangles) and the West Wandoan 1 well core analysis (circles).

3.4   Relative permeability curves for UQ-SDAAP injection models

After comparing the relative permeability data from the West Wandoan 1 well with data from Burnside and Naylor 2014, the project concluded that the relative permeability curves and endpoints used for modelling in the UQ-SDAAP project should be based mainly on the available core data. This was specific to the target formation (the Blocky Sandstone Reservoir). While the endpoint relative permeabilities to CO$_2$ were at the low end of those available in literature, they were not sufficiently low to be considered unreasonable.

UQ-SDAAP created a set of drainage relative permeability curves representing an "average" of that seen in the core data (Figure 3) for use in CO$_2$ injection simulations. This average curve was created by first fitting Brooks-Corey curves to the available water relative permeability (k_{rw}) data from the West Wandoan 1 core analysis. These curves are based on the equation:

$$k_{rw} = \left(\frac{S_w - S_{wr}}{1 - S_{wr}}\right)^{\frac{2+3\lambda}{\lambda}}$$

(Brooks and Corey 1964), where k_{rw}, S_w and S_{wr} are as defined previously, and λ is related to the distribution of pore throat sizes (higher values of λ indicate narrower distributions of pore throat size). Curves were fit to the available date using the lowest recorded S_w value for each curve as S_{wr}, and then adjusting λ to minimise the square error. In cases where it was possible to fit the curves using this method, λ was between 0.55 and 3.28, with a mean of 1.31. An estimated "average" k_{rw} curve was created using this average value for λ (1.31), along with the average S_{wr} for all plugs (0.49). An equivalent k_{rg} curve was created based on the Brooks-Corey equation:

$$k_{rg} = \left(\frac{1 - S_w}{1 - S_{wr}}\right)^2 \left[1 - \left(\frac{S_w - S_{wr}}{1 - S_{wr}}\right)^{\frac{2+\lambda}{\lambda}}\right]$$

This curve was then scaled to match the average of the maximum kr$_g$ values (0.126) at S_{wr}.

Figure 3 *Relative permeability curves from West Wandoan 1 plugs are shown as thinner lines in both plots. (A) Initial drainage relative permeability curves (thick dashed lines) using average values for λ, S_{wr} and maximum k_{rg}. (B) Rescaled drainage relative permeability curves (thick solid lines) using adjusted values for λ, S_{wr} and maximum k_{rg}, to account for limitations of laboratory experiments and capillary pressure modelling effects in simulations (see section 4.3). Note that curves are <u>almost</u> identical up to $S_w = 0.5$.*
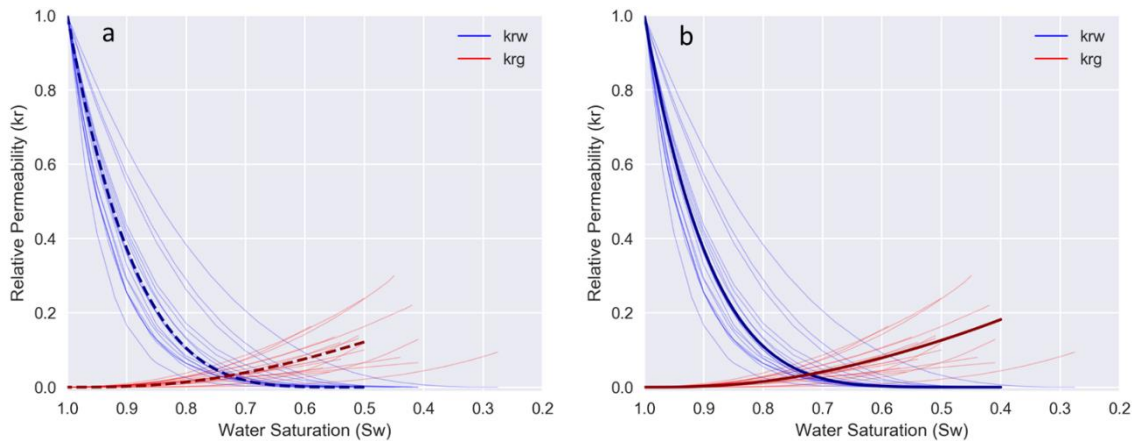
Based on the limitations of the laboratory experiments where *"measured data do not fully represent the endpoints"* (ANLEC 2016), UQ-SDAAP deemed it necessary to extend the curves to slightly lower values of S_{wr} to allow the numerical simulations to better represent the multiphase behaviour of the CO_2-water system in the Blocky Sandstone Reservoir. This also allowed the use of capillary pressure functions, which included a "steeper" increase in capillary pressure at close to S_{wr} (discussed further in section 4.3). Conceptually, this allows us to represent a case where if sufficiently high pressure is reached, water saturations in the simulations could be reduced beyond the average S_{wr} achieved in laboratory experiments. This can be limited by low displacement pressures.

While extending the k_{rw} and k_{rg} curves, UQ-SDAAP wanted them to (approximately) retain the shape they had in the range of saturations the laboratory experiments identified. For this reason, the values of S_{wr}, λ and maximum k_{rg} were adjusted to 0.41, 0.80 and 0.18. These values were all within the ranges for the West Wandoan core measurements, and the resulting curves (Figure 3 B) were considered a reasonable reference case. These curves are drainage curves representing the behaviour of the CO_2-water system when the saturation of the wetting phase (in this case water) is decreasing. Imbibition curves were not specifically defined for the UQ-SDAAP dynamic models. Instead, the HYSKRG keyword in GEM was used to define the maximum residual gas[3] saturation. This allows GEM to evaluate imbibition curves that leave the drainage curve at any saturation (i.e. even if S_{wr} is not reached) to be determined as described in the CMG GEM manual. Based on the available data from West Wandoan 1 (where most samples had residual CO_2 saturations between 0.25 and 0.4) we estimated that a value of 0.35 was a reasonable reference case value for the residual saturation of CO_2.

The project was unable to find any measured data on the relative permeability of the CO_2-water system in the Transition Zone or Ultimate Seal, the same curves were used for these zones as for the Blocky Sandstone Reservoir.

There remains significant uncertainty around the relative permeability of the CO_2-water system in the Blocky Sandstone Reservoir in the deeper parts of the Surat Basin, and in the Transition Zone and Ultimate Seal. This uncertainty cannot be reduced unless an appraisal well is drilled to allow dynamic testing and special core analysis (SCAL). While we cannot currently reduce the uncertainty, we can use models to test the sensitivity of a notional injection scenario to these properties. To test the effect of relative permeability on

---

[3] "Gas" is used here as the CMG manual refers to the non-aqueous phase as gas. In this case it refers to supercritical CO_2.

injectivity, residual CO_2 saturation and plume spread, the end points of these "reference case" curves were scaled within CMG's GEM software to represent low and high cases for:

A. Residual water saturation (S_{wr}): low = 0.25, high = 0.55

B. Maximum permeability to CO_2 (k_{rgmax}): low= 0.10, high = 0.30

C. Residual CO_2 saturation (S_{rCO2}): low = 0.20, high = 0.50

The selection and use of these values is discussed further in Rodger et al. 2019f.

4.   Capillary pressure

4.1   Background

Capillary pressure is the difference in pressure across the interface between two immiscible fluids caused by capillary forces. If we consider an oil/water system in a single capillary tube the capillary pressure can be calculated using the Young-Laplace equation:

$$p_{oil} - p_{water} = P_c = \frac{2\sigma \cos \theta}{r}$$

where p is the phase pressure, P_c is capillary pressure, σ (in some literature γ) is the interfacial tension, θ is the wetting angle of the liquid on the solid surface (which indicates the wettability of the system), and r is the radius of the capillary tube. It is important to note that increasing r (the radius of the capillary tube) will decrease the capillary pressure.

The pore network in a rock can be considered similar to a complex combination of capillary tubes. As a non-wetting phase is injected at a specific pressure it will only enter pores where r is greater than the value of r which equates to that specific pressure based on the Young-Laplace equation. In essence, for any pressure there exists a threshold pore radius, and pore throats smaller than this threshold cannot be entered by the non-wetting phase. This limits the saturation of the non-wetting phase at any specific pressure. If the pressure is increased, the threshold radius decreases and the saturation of the non-wetting phase will increase. The capillary pressure curve for a pair of fluids in a rock sample indicates how the pressure and saturation is related. The shape of this curve will be dependent on a number of factors, including σ, θ, and the distribution of pore throat sizes in the rock.

Capillary pressures are particularly important when considering the behaviour of the CO_2-water system in the Transition Zone and Ultimate Seal if CO_2 is the non-wetting phase. Seals in hydrocarbon bearing formations, where the hydrocarbon is the non-wetting phase, are often membrane seals. Migration of hydrocarbons is prevented by capillary effects rather than simply by low leakage rates, as is the case for hydraulic seals. Membrane seals can fail, allowing hydrocarbons to migrate through them if the capillary threshold pressure is exceeded. This is the pressure at which "a continuous thread of non-wetting fluid extends across the sample" (Underschultz 2007). The threshold pressure will be slightly higher than the capillary entry pressure. This is the pressure at which the largest pore throats are entered. While the non-wetting phase could *enter* a seal at the capillary entry pressure, it could not pass *through* until the threshold pressure is reached. Often seal capacity is estimated by calculating the height of a column of fluid (e.g. oil or gas) which would cause the pressure due to the buoyancy of the hydrocarbon to equal the threshold pressure of the seal. In essence, this would be the point where any further increase of the column height would raise the pressure beyond the threshold pressure and cause the membrane seal to fail.

In order to reasonably represent the behaviour of CO_2 in UQ-SDAAP injection models, the project needed to identify a method of approximating the capillary pressure curves that would be expected for the Blocky Sandstone Reservoir, Transition Zone and Ultimate Seal.

4.2 Capillary pressure data from the Blocky Sandstone Reservoir, Transition Zone and Ultimate Seal
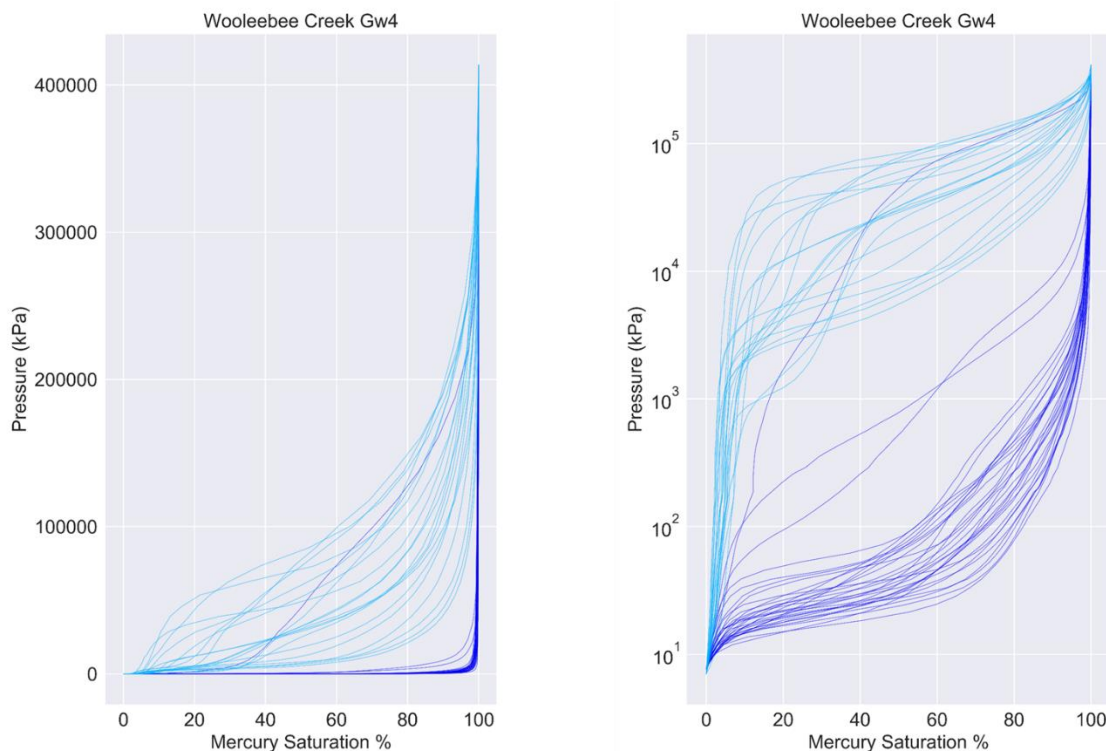
Relevant capillary pressure data was available from three wells:

- MICP data, including raw data, from Moonie 12 (Transition Zone only)

- MICP data, including raw data, from Woleebee Creek GW 4 (all three zones).

- CO$_2$/brine plots and analysis from West Wandoan 1 SCAL (Blocky Sandstone Reservoir only)

The data from Moonie 12 was a seal capacity report that had been used to determine whether or not the "seal" in the Moonie field (which is considered part of the Transition Zone in the UQ-SDAAP scheme), had sufficiently high threshold pressure that hydrocarbons would "spill" out of the Moonie anticline before a membrane seal failure occurred. Three core samples were analysed using MICP analysis, which indicated air/mercury threshold pressures of 15,396kPa, 42,147kPa and 48,332kPa, equivalent to seal capacities of 319m, 953m and 1100m of oil. The capillary pressure curves from Moonie 12 were not used directly in creating the curves used in the UQ-SDAAP numerical simulations, but are reported here to allow comparison.

Extensive MICP data from all three zones was available from Woleebee Creek GW4 and used as the basis for estimating capillary pressure curves which would be used in the UQ-SDAAP Models. The MICP curves from this well are shown in Figure 4. Air-mercury threshold pressures for the Blocky Sandstone Reservoir were typically between 12.5kPa and 25kPa, while the Transition Zone and Ultimate Seal threshold pressures were <u>much</u> higher, ranging from 1,100kPa to 63,000kPa. These higher were consistent with the results from Moonie 12. The Woleebee Creek GW4 data, and a description of how it was used to create input curves for UQ-SDAAP models, is discussed in more detail in Section 4.3.

Figure 4   MICP data from Woleebee Creek GW4. Both plots show same data, but right side plot has log scale for pressure. Dark blue lines are data from "Precipice Sandstone" (Blocky Sandstone Reservoir) while light blue lines are from "Evergreen Formation" (Transition Zone/Ultimate Seal).

Some CO_2-brine capillary pressure data for the Blocky Sandstone Reservoir was available from the SCAL reports for West Wandoan 1 (the same analysis which provided relative permeability data). Capillary pressure curves were fit to the experimental data based on the Van Genuchten model:

$$P_c = P_e \left(\left(\frac{S_w - S_{wr}}{1 - S_{wr}} \right)^{1/\lambda} - 1 \right)^{(1-\lambda)}$$

where S_{wr} is the residual water saturation, P_e represents the entry pressure, and λ alters the curvature (similar to the λ term in the Brooks Corey equation shown in Section 0). The report on this analysis indicates the best fit for most plugs was achieved using P_e = 1.72kPa, S_{wr} = 0.26 and λ = 0.4. The experimental data was scattered. Higher permeability plugs (greater than 2000mD) needed higher values of λ for the Van Genuchten model to fit the data, but all models used P_e less than 17.5kPa (ANLEC 2016).

4.3   Capillary pressure curves for UQ-SDAAP injection models

The MICP data available from Woleebee Creek GW4 and the CO_2-brine data from West Wandoan 1 both indicated variability of capillary pressures occur within the Blocky Sandstone Reservoir, with even more variability in the Transition Zone and Ultimate Seal in the Woleebee Creek GW4 well. This is unsurprising due to the geologically heterogeneous nature of the Transition Zone in particular. For this reason, UQ-SDAAP decided to make use of J functions to represent the capillary pressure curves for both the Blocky Sandstone Reservoir and Transition Zone/Ultimate Seal.

The J functions used in the UQ-SDAAP models are based on the premise that capillary pressures for similar rocks can be related to the porosity (ϕ) and permeability (k) of a rock based on the equation:

$$P_c = 798 \times J_{(Sw)} \times \sqrt{\left(\frac{\phi}{k} \right)}$$

where $J_{(Sw)}$ is the value of the defined J function for the specified rocktype at a specified saturation (S_w or S_{CO2}). The factor preceding the J term can be varied within the dynamic model grid to represent spatially varying surface tension and contact angles, however in the UQ-SDAAP models these values were considered constant.

The use of J functions would allow the project to have spatially variable capillary pressure curves (which would be based on the porosity and permeability of individual grid blocks in the model). This was considered particularly important when modelling the Transition Zone, which is expected to be very heterogeneous. If a single capillary pressure curve was used for the Transition Zone, CO_2 would enter any cells when a specified entry pressure was reached. UQ-SDAAP deemed this unlikely due to the heterogeneous nature of the Transition Zone, and considered it probable that CO_2 would migrate into the Transition Zone in 'sandier' areas, where permeability was likely higher, and capillary pressure lower, but not in 'shalier' parts where the opposite is true. This variability could be captured if a J function was used in place of a single capillary pressure curve in the dynamic model.

The J functions for the UQ-SDAAP models were based mainly on the data from Woleebee Creek GW4, as this well had extensive data available in both the Blocky Sandstone Reservoir and Transition Zone/Ultimate Seal. To create these functions from the available MICP data, the first step was to convert the mercury-air capillary pressure values to CO_2-water pressures according to:

$$P_{cw} = \frac{\sigma_{cw} \cos \theta_{cw}}{\sigma_{ma} \cos \theta_{ma}} \times P_{ma}$$

where the subscripts *ma* and *cw* indicate the values for the mercury-air and CO_2-water systems. To use these calculations, UQ-SDAAP needed to estimate values for the interfacial tension (σ) and contact angle (θ) for the CO_2-water system. The values used were: σ_{cw}= 28.5dynes/cm σ_{ma} = 481 dynes/cm, θ_{cw} =50 degrees, and θ_{ma}=140 degrees. There remains significant uncertainty in these estimates in particular, as the contact angle (i.e. wettability) and interfacial tension of the CO_2-water system varies with temperature, pressure,

mineralogy, organic content and salinity, amongst other things. The value for the contact angle used was based on high pressure (10Mpa) values reported in Daniel and Kaldi 2008, and similar values in Iglauer et al. 2014. The Interfacial tension value was an estimate based on the summaries presented in Chiquet et al. 2007. Again, these values are estimates only, and remain a significant source of uncertainty.

Using the estimated values specified above, we calculated the CO_2-water capillary pressure as:

$$P_{cw} = 0.05 \times P_{ma}$$

We then calculated J values for each saturation using the porosity and permeability data for each sample and the equation:

$$J_{(Sw)} = \frac{P_c}{798\sqrt{\left(\frac{\phi}{k}\right)}}$$

The resulting capillary pressure and J function curves for the Woleebee Creek GW4 samples are shown in Figure 5.

Figure 5   *(A) Calculated CO_2-water capillary pressure curves for the Woleebee Creek GW4 well samples (B) Calculated J functions based on 'a'. Dark blue lines are samples from the Blocky Sandstone Reservoir, while lighter blue lines are from the Transition Zone/Ultimate Seal samples.*
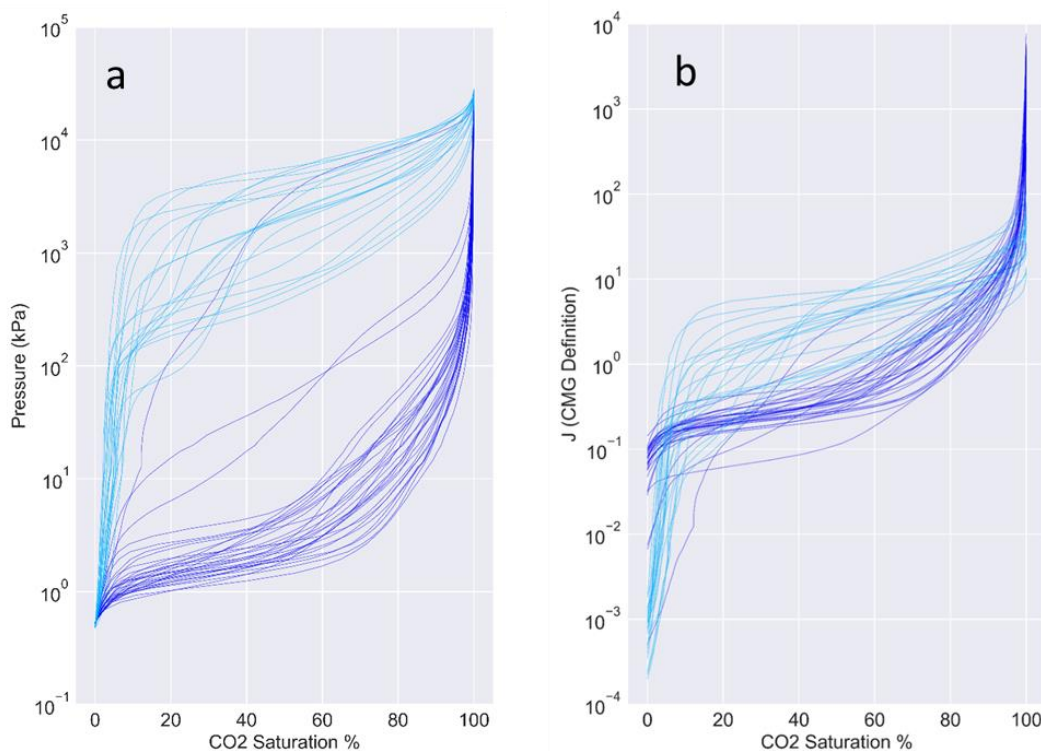
Initially, UQ-SDAAP attempted to use a single J function to represent all of these samples, but this appeared to cause underestimation of the capillary pressures in the Transition Zone and Ultimate Seal, and overestimation of the capillary pressures in the Blocky Sandstone Reservoir, when the capillary pressure curves were recalculated using the J functions and the porosity/permeability values from the Woleebee Creek GW 4 well samples. For this reason, we decided it would be more appropriate to use two curves: one for the Blocky Sandstone Reservoir, and one for the Transition Zone/Ultimate Seal. The defined curves are shown in Figure 6 (A), along with the resulting capillary pressure curves (B) and (C). These curves were calculated using the porosity/permeability values from the Woleebee Creek GW 4 samples.

*Figure 6   (A) J functions used for the Blocky Sandstone Reservoir (solid red) and Transition Zone/Ultimate Seal (dashed red) in UQ-SDAAP models overlain on the J functions calculated from the Woleebee Creek GW 4 Samples (as shown in **Error! Reference source not found.** (B). (B) Capillary pressure curves calculated using the curves in 'a', and porosity/permeability values from the Woleebee Creek GW 4 well samples. Orange/Red curves are Transition Zone/Ultimate Seal and Blue/Green are Blocky Sandstone Reservoir, (C) The same curves as in b overlain on the original capillary pressure curves.*
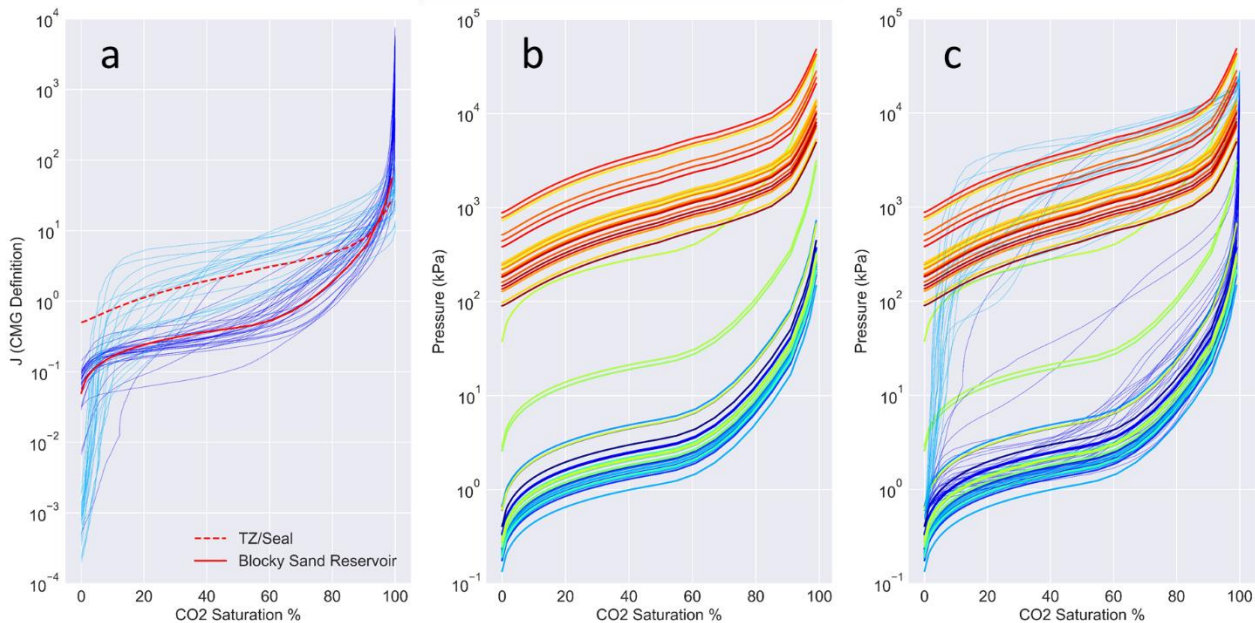
Figure 6 indicates that the J functions specified provide a reasonable range of capillary pressure curves when compared to the range of curves calculated from the MICP data. One important feature of the defined J function used for modelling of the Transition Zone/Ultimate Seal is that it does not decline sharply below approximately 10% CO_2 saturation. This feature is present in the J functions calculated from the MICP data, and coincides with a similar feature in the measured capillary pressures.

The reason this was not included in the J function for the Transition Zone/Ultimate Seal used in the UQ-SDAAP models was that the low capillary pressures (below 10% mercury saturation) would be caused by mercury entering the largest pores in the sample. The mercury could enter the edge of the sample, but could not flow through it unless a connected network of sufficiently large pores existed. This is important when considering the scale of the grid blocks used in the UQ-SDAAP models, in particular in the Transition Zone. While CO_2 could perhaps "enter" the Transition Zone by moving into the largest pores at the interface between the Transition Zone and the Blocky Sandstone Reservoir, it would not be able to move further through due to heterogeneity, and thus the CO_2 saturation of the large grid block would remain low.

In the models using a J function curve that included low values at low CO_2 saturations, the simulator would allow CO_2 to enter the Transition Zone at low pressures. As this saturation would be 'dispersed' throughout the grid block (the saturation is averaged, not specifically located at the bottom of the block), this would "artificially" create a situation where CO_2 might appear to migrate through the Transition Zone even if the threshold capillary pressure had not been reached. This was not considered as important for the Blocky Sandstone Reservoir where the capillary pressures are expected to be much lower.

The resulting J functions were scaled to match the residual water saturation (S_{wr} = 0.4 for the reference case) from the West Wandoan relative permeability data. The curves were scaled this way so they could be later rescaled within the CMG GEM software for sensitivity analysis. This would also mean that the maximum saturation of CO_2 reached could be dependent on the porosity and permeability of the cell (due to the effect of rapidly increasing capillary pressures near the defined value of S_{wr}).

There is significant uncertainty around the capillary pressure behaviour of the Blocky Sandstone Reservoir, Transition Zone and Ultimate Seal. Also, the functions defined to represent the capillary pressures are not likely to be accurate. We consider them a reasonable approximation for use in the reference case in notional injection modelling. Alternate capillary pressure curves will be defined in the sensitivity analysis part of the project to provide some indication of the impact that these curves have on injectivity, plume spread, and CO_2 trapping. Studies (e.g. Iglauer et al. 2015) suggest mudrocks could be intermediate-wet or even CO_2-wet. As the majority of the Transition Zone is considered to be mudrock (with varying mineralogy and properties), a case with no capillary entry pressure will be used in a sensitivity study to test the scenario where the Transition Zone is intermediate-wet or CO_2-wet.

Ultimately, this uncertainty needs to be reduced through SCAL of core from the Blocky Sandstone Reservoir, Transition Zone and Ultimate Seal near the area identified as a notional injection site.

5.   Conclusions

Limited relative permeability data is available for the Blocky Sandstone Reservoir, Transition Zone and Ultimate Seal in the UQ-SDAAP study area. The available data suggests that the Blocky Sandstone Reservoir is likely to have lower relative permeability to CO_2 compared to other analogous sandstones described in the literature, which may limit injectivity.

Capillary pressure data is particularly important in the Transition Zone as it determines, in part, whether or not CO_2 is likely to migrate vertically during and after injection. The available data suggests that some parts of the Transition Zone act as a good membrane intra-formational seal, as seen in the Wooleebee Creek GW4 and Moonie 12 wells. However, it is unclear how representative these samples are of the Transition Zone across the Surat Basin, and particularly in the areas identified as notional injection sweet-spots. The Transition Zone in the Woleebee Creek GW4 well has generally very low permeability (typically <0.1md, and in some cases reported as 0.00md or "N/A"), and thus may indicate higher capillary pressures than would be seen elsewhere in the basin. Note that core sampling of the Moonie 12 well was targeting a seal, and thus samples were likely biased towards high capillary pressures.

It is important to realise that a raft of independent evidence from the MAR injection, regional geological analyses, hydrogeology and reviews of Moonie and other hydrocarbon accumulations are consistent with an interpretation of Transition Zone which when taken as a whole will form a significant barrier to vertical flow (Garnett et al. 2019). It should also be noted that the Ultimate Seal is laterally continuous and lithologically consistent from West to East and across the majority of the Basin.

Ultimately, we have used the available data to create relative permeability and capillary pressure curves that capture the range of uncertainty and are used as a reasonable reference case and range for sensitivity analysis for the notional injection models, although we acknowledge that there are remaining large uncertainties regarding these curves and the parameters (such as contact angle and interfacial tension) that affect them.

The uncertainties that have been identified cannot be reduced without new SCAL of core from the Blocky Sandstone Reservoir, Transition Zone and Ultimate Seal near the area identified as a notional injection site.

6.   References

ANLEC (2016), Milestone 1.4 Final report of RCA and SCAL data on plugs from West Wandoan-1 Well. Lithicon, Canberra.

Bachu S (2013), Drainage and Imbibition CO2/Brine Relative Permeability Curves at in Situ Conditions for Sandstone Formations in Western Canada, *Energy Procedia*, vol 37, pp 4428-4436.

Bennion B & Bachu S (2008), Drainage and Imbibition Relative Permeability Relationships for Supercritical CO2/Brine and H2S/Brine Systems in Intergranular Sandstone, Carbonate, Shale, and Anhydrite Rocks. *SPE Reservoir Evaluation & Engineering*, vol 11, pp 487-496.

Brooks RH & Corey AT (1964), Hydraulic properties of porous media, *Hydrology papers* (Colorado State University), no 3.

Burnside NM & Naylor M (2014), Review and implications of relative permeability of CO2/brine systems and residual trapping of CO2, *International Journal of Greenhouse Gas Control*, vol 23, pp 1-11.

Chiquet P, Daridon J-L, Broseta D et al. (2007), CO2/water interfacial tensions under pressure and temperature conditions of CO2 geological storage, Energy Conversion and Management, vol 48, pp 736-744.

Daniel R and Kaldi J (2008), Evaluating seal capacity of caprocks and intraformational barriers for the geosequestration of CO2.

Garnett AJ, Underschultz JR & Ashworth P (2019), *Project Report: Scoping study for material carbon abatement via carbon capture and storage*, The University of Queensland Surat Deep Aquifer Appraisal Project, The University of Queensland.

Gonzalez S, He J, Underschultz J & Garnett A (2019), *Seismic interpretation - geophysics*, The University of Queensland Surat Deep Aquifer Appraisal Project – Supplementary Detailed Report, The University of Queensland.

Gonzalez S, Harfoush A, La Croix A, Underschultz J & Garnett A (2019*), Regional static model*, The University of Queensland Surat Deep Aquifer Appraisal Project – Supplementary Detailed Report, The University of Queensland.

Honarpour M & Mahmood SM (1988), Relative-Permeability Measurements: An Overview, *Journal of Petroleum Technology*, vol 40, pp 963-966.

Harfoush H, Altaf I & Wolhuter A (2019), *Wireline log analysis*, The University of Queensland Surat Deep Aquifer Appraisal Project – Supplementary Detailed Report, The University of Queensland.

Harfoush A, Pearce J & Wolhuter A (2019), *Core data analysis*, The University of Queensland Surat Deep Aquifer Appraisal Project – Supplementary Detailed Report, The University of Queensland.

Harfoush A, Hayes P, La Croix A, Gonzalez S & Wolhuter A (2019), *Integrating petrophysics into modelling*, The University of Queensland Surat Deep Aquifer Appraisal Project – Supplementary Detailed Report, The University of Queensland.

Harfoush A, Gonzalez S, Ribeiro A & Wolhuter A (2019), *Fluid substitution for seismic detection of plume*, The University of Queensland Surat Deep Aquifer Appraisal Project – Supplementary Detailed Report, The University of Queensland.

Iglauer S, Sarmadivaleh M, Lebedev, M, Vogt S, AlYaseri A.Z, Arif M, Ahmed S, Geng C, Coman C, Rahman T, Haugen P, Ferno M, Johns M (2014*), Pore and core-scale investigation of CO2 mobility, wettability and residual trapping*, Curtin University.

Iglauer S, Pentland C H & Busch A (2015), CO2 wettability of seal and reservoir rocks and the implications for carbon geo-sequestration, *Water Resources Research*, vol 51(1), pp 729-774.

Krevor SCM, Pini R, Zuo L et al. (2012), Relative permeability and trapping of CO2 and water in sandstone rocks at reservoir conditions, *Water Resources Research*, vol 48.

La Croix A, Wang J & Underschultz J (2019*), Integrated facies analysis of the Precipice Sandstone and Evergreen Formation in the Surat Basin*, The University of Queensland Surat Deep Aquifer Appraisal Project – Supplementary Detailed Report, The University of Queensland.

La Croix A, Wang J, Gonzalez S, He J, Underschultz J & Garnett A (2019), *Sequence stratigraphy of the Precipice Sandstone and Evergreen Formation in the Surat Basin*, The University of Queensland Surat Deep Aquifer Appraisal Project – Supplementary Detailed Report, The University of Queensland.

La Croix A, He J, Wang J & Underschultz J (2019), *Facies prediction from well logs in the Precipice Sandstone and Evergreen Formation in the Surat Basin*, The University of Queensland Surat Deep Aquifer Appraisal Project – Supplementary Detailed Report, The University of Queensland.

La Croix A, Hannaford C & Underschultz J (2019), *Palynological analysis of the Precipice Sandstone and Evergreen Formation in the Surat Basin*, The University of Queensland Surat Deep Aquifer Appraisal Project – Supplementary Detailed Report, The University of Queensland.

Pentland CH, El-Maghraby R, Georgiadis A et al. (2011), Immiscible Displacements and Capillary Trapping in CO2 Storage, *Energy Procedia,* vol 4, pp 4969-4976.

Perrin J-C & Benson S (2010), An Experimental Study on the Influence of Sub-Core Scale Heterogeneities on CO2 Distribution in Reservoir Rocks, *Transport in Porous Media*, vol 82, pp 93-109.

Rodger I, Harfoush A & Underschultz J (2019), *CO_2 injection sensitivity study*, The University of Queensland Surat Deep Aquifer Appraisal Project – Supplementary Detailed Report, The University of Queensland.

Satter A, Iqbal GM & Buchwalter JL (2008), *Practical enhanced reservoir engineering: assisted with simulation software*, Pennwell Books.

Shi J-Q, Xue Z & Durucan S (2011a), Supercritical CO2 core flooding and imbibition in Berea sandstone — CT imaging and numerical simulation, *Energy Procedia*, vol 4, pp 5001-5008.

Shi J-Q, Xue Z and Durucan S (2011b), Supercritical CO2 core flooding and imbibition in Tako sandstone—Influence of sub-core scale heterogeneity, *International Journal of Greenhouse Gas Control*, vol 5, pp 75-87.

Underschultz J (2007), Hydrodynamics and membrane seal capacity, *Geofluids*, vol 7, pp 148-158.